Dalton Transactions

ROYAL SOCIETY OF CHEMISTRY

COMMUNICATION

View Article Online
View Journal | View Issue

Cite this: *Dalton Trans.*, 2024, **53**, 17789

Received 3rd October 2024,
Accepted 18th October 2024

DOI: 10.1039/d4dt02791d

rsc.li/dalton

Unprecedented C–F bond cleavage in perfluoronaphthalene during cobaltocene reduction†

Gargi Kundu,[a,b] Debjit Pramanik,[a,b] Soumya Ranjan Dash,[b,c] Ravi Kumar,[b,c] Mayur Sangole,[b,c] Srinu Tothadi,[b,d] Aryya Ghosh,*[e] Kumar Vanka,*[b,c] Kirandeep Singh*[b,c] and Sakya S. Sen*[a,b]

The C–F bond activation of perfluoronaphthalene by 5-SIDipp led to the formation of dicationic salts with two fluorides (3·2HF$_2$) or heptafluorodiborate (3·2B$_2$F$_7$) as counter-anions. The anion exchange reaction of 3·2B$_2$F$_7$ with NBu$_4$PF$_6$ afforded a highly luminescent 3·2PF$_6$. The *in situ* addition of cobaltocene in the reaction mixture of 5-SIDipp and perfluoronaphthalene led to a distinct Co(I) species.

Seminal works from Ghadwal and Jana *et al.* resulted in carbene-based Thiele, Tschitschibabin and Müller hydrocarbons.[1,2] We have recently accessed such Kekulé diradicaloids with perfluoroarene spacers and attempted to understand the impact of fluoride substitution on their diradical character. We have isolated imidazoline-2-ylidene-based Thiele's and Tschichibabbin's hydrocarbons with a tetrafluorophenylene linker, where the replacement of hydrogen atoms by fluorine atoms reduces the singlet–triplet gap.[3,4]

The spacer in these diradicaloids has been restricted to either the phenylene or biphenylene group. Notable exceptions came from the groups of Bertrand and Masuda, who independently reported the synthesis of organic Kekulé diradicaloids having a 1,4-diethynylphenyl spacer with *c*AACs or imidazoline-2-ylidene, respectively.[5,6] Recently, Aldridge and coworkers reported organoboron analogues of Thiele's hydrocarbon using a pyridine spacer.[7] While there are some reports on diradicaloids with fused rings,[8,9] their stabilization with carbenes is unprecedented in the literature. We commenced our study with a naphthalene spacer inspired by the works of the groups of Chi and Haley for developing novel π-structures and synthesis of high-performance conjugated materials using a 2,6-naphthoquinodimethane core.[9] Our endeavours in isolating a perfluoronaphthalene-based Kekule diradicaloid led to an unusual Co(I) complex.

The reaction of two equivalents of 5-SIDipp (**1**) with one equivalent of octafluoronaphthalene (**2**) in hexane under ambient conditions resulted in a red-coloured precipitate *via* NHC-mediated C–F bond activation,[10] which was isolated as the dicationic fluoride salt **3·2HF$_2$**. Unfortunately, due to low solubility, we were unable to characterize **3·2HF$_2$** by NMR spectroscopy, but its formation was confirmed by a single crystal X-ray study (Fig. 1). The addition of two equivalents of BF$_3$·ether into the reaction mixture resulted in the dicationic heptafluorodiborate salt **3·2B$_2$F$_7$** (Scheme 1 and Fig. 2), which was characterized by ^{11}B NMR (δ −1.5 ppm) and ^{19}F NMR (δ −148.3 ppm) spectroscopy. The molecular ion peak at *m*/*z* 507.2983 in the HRMS supported the formation of **3·2B$_2$F$_7$**. The molecular structures of **3·2HF$_2$** and **3·2B$_2$F$_7$** were determined by single crystal X-ray diffraction studies, with the important bond lengths and angles given in the legends of the respective figures.

The reaction of **3·2B$_2$F$_7$** with NBu$_4$PF$_6$ underwent a huge color change and resulted in the anion exchange product **3·2PF$_6$** (Scheme 1). The ^{31}P NMR spectrum shows a signal at −144.4 ppm and the ^{19}F NMR spectrum exhibits signals at −72 ppm and −73.9 ppm characteristic of the PF$_6$ anion and −151.9 ppm for the aromatic six fluorine atoms. While the X-ray analysis unequivocally confirms the constitution of **3·2PF$_6$**, one of the PF$_6$ moiety is highly disordered and hence masked during the refinement. Despite several attempts, the data quality is very poor as R_{int} is >25. Hence, we refrain from discussing the crystal structure and have provided the molecular structure only in the ESI (See Fig. S25).† After observing a strong visible luminescence under UV irradiation, we studied

[a]*Inorganic Chemistry and Catalysis Division, CSIR-National Chemical Laboratory, Dr Homi Bhabha Road, Pashan, Pune 411008, India. E-mail: ss.sen@ncl.res.in*
[b]*Academy of Scientific and Innovative Research (AcSIR), Ghaziabad 201002, India*
[c]*Physical and Materials Chemistry Division, CSIR-National Chemical Laboratory, Dr. Homi Bhabha Road, Pashan, Pune 411008, India. E-mail: k.vanka@ncl.res.in, kp.singh@ncl.res.in*
[d]*Analytical and Environmental Sciences Division and Centralized Instrumentation Facility, CSIR-Central Salt and Marine Chemicals Research Institute, Gijubhai Badheka Marg, Bhavnagar-364002, India*
[e]*Department of Chemistry, Ashoka University, Sonipat, Haryana 131029, India. E-mail: aryya.ghosh@ashoka.edu.in*

†Electronic supplementary information (ESI) available: Experimental details, crystallographic details, and the relevant spectroscopic data. CCDC 2270083 (**3·2HF$_2$**), 2270084 (**3·2B$_2$F$_7$**) and 2270085 (**5**). For ESI and crystallographic data in CIF or other electronic format see DOI: https://doi.org/10.1039/d4dt02791d

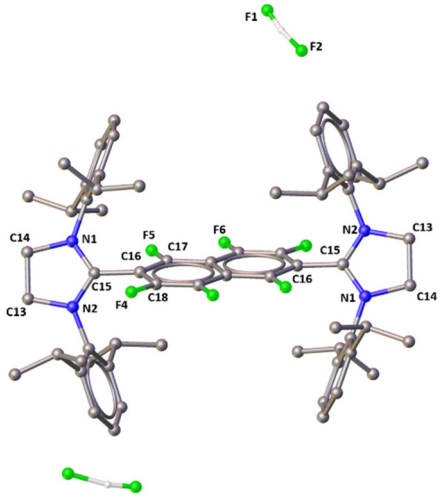

Fig. 1 Molecular structure of **3·2HF$_2$**. Hydrogen atoms are omitted except for the HF$_2$- anions for clarity. Selected bond distances (Å) and angles (°): C15–N1 1.316(3), C15–N2 1.320(3), C14–N1 1.487(3), C13–N2 1.488(3), C15–C16 1.483(3), C17–F5 1.299(3); N1–C15–N2 113.97(18), C13–N2–C15 109.49(17), N1–C15–C16 109.70(17), N2–C15–C16 124.23 (19); N1–C15–C16–C17 54.9(3), N2–C15–C16–C18 58.3(3).

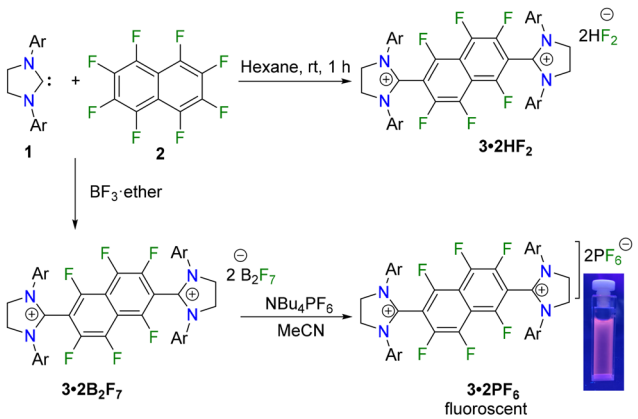

Scheme 1 Synthetic access to dicationic salts (**3·2HF$_2$**, **3·2B$_2$F$_7$** and **3·2PF$_6$**) with a perfluoro-substituted naphthalene spacer (Ar = 2,6-iPr$_2$-C$_6$H$_3$).

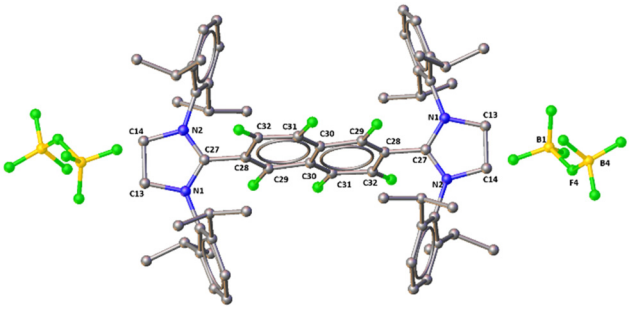

Fig. 2 Molecular structure of **3·2B$_2$F$_7$**. Hydrogen atoms are omitted for clarity. Selected bond distances (Å) and angles (°): C27–N1 1.312(6), C27–N2 1.324(6), C27–C28 1.491(7), C28–C29 1.275(9), C29–C30 1.519 (10), C28–C32 1.541(9), C32–C31 1.453(8), C31–C30 1.340(9); N1–C27–N2 113.3(4), N1–C27–C28 122.0(4), N2–C27–C28 124.6(4), B1–F4–B2; N1–C27–C28–C32 63.1(7), N1–C27–C28–C29 –114.0(7), N2–C27–C28–C29 68.3(9), N2–C27–C28–C32 –114.6(6).

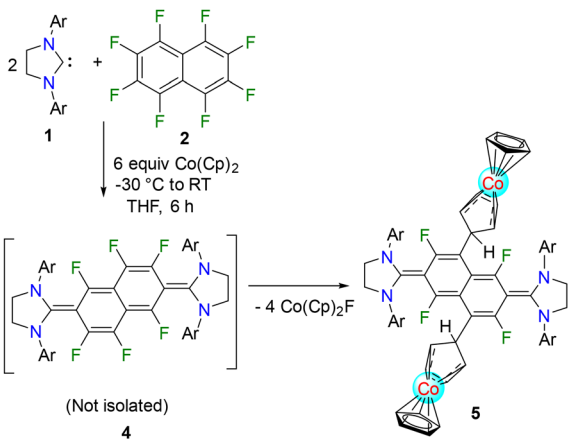

Scheme 2 Synthetic access to fluoro-substituted naphthalene spacer-based Kekulé diradicaloid, **5**.

the photo-physical phenomenon of **3·2PF$_6$**, which shows two very intense absorptions bands at 370 nm and 485 nm. Upon the excitation at 370 nm and 485 nm, **3·2PF$_6$** gives a strong emission band at 629 nm (Fig. S17 and S18†). The lifetime measurement shows bi-exponential decay of **3·2PF$_6$** with lifetimes τ_1 = 0.91 ns (83.92%) and τ_2 = 9.59 ns (16.08%) (χ^2 = 0.9975124), which is indicative of prompt fluorescence (Fig. S19†).

The one pot reaction of 5-SIDipp, octafluoronaphthelene with cobaltocene at −30 °C temperature in THF, led to the unprecedented formation of **5**, presumably *via* the formation of intermediate **4** (Scheme 2). The formation of **5** was observed regardless of the equivalents of cobaltocene. In **5**, two *meta*-C–F bonds of the naphthalene moiety have been replaced by cobaltocene and form two C–C bonds. While the C–F bond activation by Co complexes has been known,[11] such activation in cobaltocene is not reported. One of the cyclopentadienyl rings, which connects with the *meta* carbon of the naphthyl ring, lost the planarity and was bound at the cobalt atom. The formal oxidation state of Co in compound **5** is +1, and it is an 18-electron species. In 2017, Bertrand and co-workers have shown the insertion of one of the Cp rings of cobaltocene in the alkyne salt to trap the radical in the reduction with cobaltocene.[12] Unfortunately, our efforts to selectively reduce **3·2HF$_2$** and **3·2B$_2$F$_7$** using cobaltocene to obtain **4** have also been unsuccessful. Attempts to characterize **5** *via* ^{1}H and ^{13}C NMR spectroscopy only result in a broad spectrum due to the presence of monoradical impurities, which is known in the literature.[1] At 260 K, small broad signals corresponding to the 5-SIDipp fragments were observed in the ^{1}H NMR spectrum of **5** in toluene-d$_8$ (Fig. S9†), while those in the ^{13}C NMR spectrum were silent (Fig. S10†). This could mean either that it exhibits a paramagnetic ground state, that they exhibit a ther-

mally populated paramagnetic excited state, or that the solutions contain a paramagnetic impurity. However, upon increasing the temperature to 298 K, the corresponding peaks at 4.67 ppm (N–CH_2CH_2–N) and 3.35 ppm (CH(CH_3)$_2$) were clearly observed for **5** (Fig. S8†). This observation suggests that **5** has a singlet ground state with a paramagnetic excited state that is populated at low temperature. We undertook variable-temperature (VT) NMR experiments for the detection of open-shell singlet ground states as the broad resonances of singlet diradical species became sharper at room temperature. In the HRMS spectrum, the peak at *m*/*z* 189.0106 is characteristic of free $CoCp_2$, which further confirms that cobaltocene is coming out from the system (Fig. S12†).

The molecular structure of **5** (Fig. 3) reveals the trigonal planar geometry at the C11/C37 carbon atom with a N3–C11–N4/N1–C37–N2 angle of 107.82(9)°/108.07(9)°. The C11–N3/N4 [1.390 Å (av)] and C37–N1/N2 [1.386 Å (av)] bond lengths are significantly longer compared to those in **3·2HF$_2$** and **3·2B$_2$F$_7$** (**3**: C15–N1/N2 1.318 Å (av), **3·2B$_2$F$_7$**: C27–N1/N2 1.318 Å (av)). The mean bond length of C11–C3/C37–C8 is 1.389 Å, which is much shorter compared to those in the dicationic salts **3·2HF$_2$** (1.483(3) Å) and **3·2B$_2$F$_7$** (1.491(7) Å). There are some bond alternations in the $C_{10}F_4$ linker across C_{ortho}–C_{ipso}, which suggests that the unpaired electrons are delocalized into the naphthyl ring (av. C_{ortho} 1.444 Å and av. C_{ipso} 1.357 Å). The imidazole rings of **5** are twisted 24.1° (av) from the plane of the bridging phenylene ring, which is substantially lower than those in **3·2HF$_2$** (56.6° (av)) and **3·2B$_2$F$_7$** (65.7° (av)), indicating a significant contribution of the quinoid resonance form in the former. The CV of **5** (Fig. S21†) revealed two reduction peaks centered at E_{red1} = −0.96 V and E_{red2} = −2.17 V *vs.* the Ag/AgCl redox couple. The peak at about −0.96 probably refers to the Co^{II}/Co^{I} couples of the cobaltocene moiety attached to the naphthalene spacer and the peak at −2.17 V possibly suggests two electron reduction or the quinoid naphthalene moiety.

DFT calculations were performed to understand the electronic structure of **5**. The optimized geometries of the singlet and triplet electronic states are shown in Fig. S25.† The singlet–triplet energy difference (ΔE_{S-T}) for compound **5** was evaluated to be 20.4 kcal mol^{-1} using the B3LYP/def2-TZVPP level of theory, which increased to 32.0 kcal mol^{-1} upon re-evaluating at the CASSCF(2,2) + CASPT2 level of theory for better accuracy (Tables S1 and S2†). It must be noted that in spite of carrying out broken-symmetry calculations, open-shell singlet structures could not be obtained for **5**. The WBI indicates a decrease in the partial double bond character of the carbene-linker (C–C) of **5** from 1.365 for the singlet to 0.272 for the triplet state.

TD-DFT calculations were also performed at the CAM-B3LYP/def2-SVP (CPCM = THF) level of theory (details in ESI†). It was revealed that the λ_{max} corresponds to the π → π* transition from the HOMO to the LUMO for **5**, where the HOMO represents the π-orbital of the naphthalene ring, which is also delocalized over the C–C linker along with the C–N bonds of each imidazolium ring, and the LUMO represents the π*-orbitals of the same molecular components, as shown in Fig. 4. Interestingly, the shoulder peak of **5** ($^{exp}\lambda$ = 461 nm) could be assigned to the mixing of two degenerate transitions: ligand to metal charge transfer and intra-ligand charge transfer (HOMO to LUMO+2, $^{calc}\lambda$ = 355 nm, f = 0.0489; HOMO to LUMO+5, $^{calc}\lambda$ = 337 nm, f = 0.0676) from the naphthalene ring to the DIPP moiety and the Co(I) center. Another peak ($^{calc}\lambda$ = 302 nm, f = 0.1478) was observed due to the presence of cobaltocene, in which the orbitals (HOMO−2 to LUMO+11) involved in the transitions were found to be delocalized on both the cobaltocenes. Consistent with the experimental observation, a

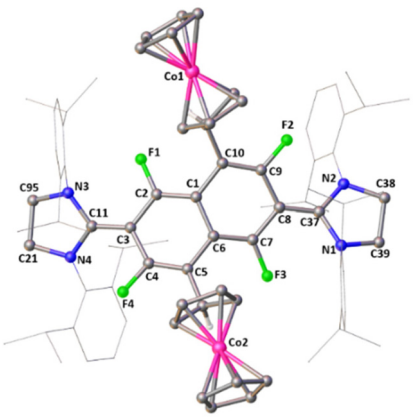

Fig. 3 The molecular structure of **5**. Hydrogen atoms, except the one hydrogen atom of the Cp ring, are omitted for clarity. Selected bond distances (Å), bond angles (°) and torsion angles (°): C11–N3 1.3912(14), C11–N4 1.3893(14), C37–N1 1.3881(14), C37–N2 1.3852(14), C11–C3 1.3897(15), C37–C8 1.3896(14), C3–C2 1.4400(15), C2–C1 1.3636(14), C1–C6 1.4610(14), C6–C5 1.3641(15), C5–C4 1.3515(15), C4–C3 1.4486(15); C2–F1 1.3589(12), C10–C70 1.5426(15), C5–C74 1.5330(16); N3–C11–N4 107.82(9), N1–C37–N2 108.07(9), N3–C11–C3 125.10(10), N4–C11–C3 127.08(10); N3–C11–C3–C2 −21.9(2), N4–C11–C3–C4 −25.5(2), N2–C37–C8–C9 −24.4(2), N1–C37–C8–C7 −24.6(2).

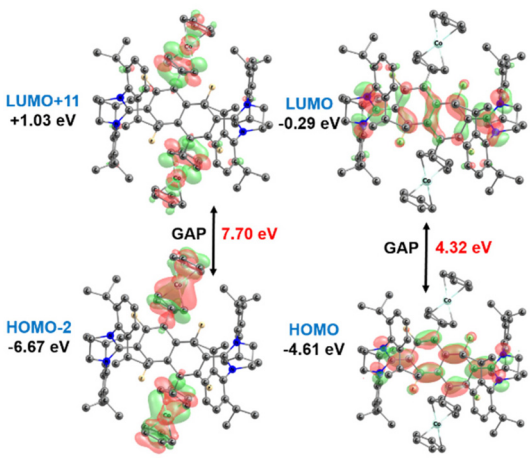

Fig. 4 Frontier molecular orbitals and their respective energies of **5** evaluated at the CAM-B3LYP/def2-SVP (CPCM = THF) level of theory. Hydrogen atoms have been omitted for clarity.

red shift in the λ_{max} values corresponding to the absorption spectrum were observed for **5** in the solution phase as compared to the gas-phase (experimental solid-state UV-Vis) TD-DFT calculations (Table S3†).

The magnetic properties of **5** were studied by recording the temperature-dependent magnetization (M–T) data in the 5–300 K temperature range (Fig. S23†) and isothermal magnetization (M–H) curves at 5 K in a cyclic ±6 T magnetic field. The magnetic susceptibility of **5** increased exponentially in the low-temperature region (below 20 K), indicating the absence of long-range ferromagnetic/anti-ferromagnetic ordering (Fig. S24†).

In addition, it is observed that both the FC and ZFC curves traced analogous paths. The inverse susceptibility data of the sample (Fig. 5) was fitted using the Curie–Weiss law, $\chi = C/(T - \theta_{CW})$, to calculate the effective magnetic moment (μ_{eff}). A μ_{eff} of nearly 4BM (BM = Bohr Magneton), which corresponds to 5 unpaired d orbital electrons, suggests that the system is abundant in free electrons. The negative value of Curie temperature "θ_{CW} to −50" signifies that the system is non-ferromagnetic in nature.[13] The absence of a hysteresis loop and saturation of magnetic moment in the M–H curves measured at 5 K (Fig. 6) again support the fact that the sample is paramagnetic in nature and is free of long-range magnetic order impurities. To gain further insight, the field dependence M–H curve was fitted with the Langevin function using the relation

$$\frac{M}{M_0} = L(a) = \coth(a) - \frac{1}{a} \quad (1)$$

where M_0 is the saturation magnetization having a value of 1.49 emu g^{-1} and $a = \mu H/kT$, μ is the effective magnetic moment and is the product of M_{bulk} and average particle volume. The M–H curve fitting to eqn (1) gives an effective magnetic moment value $\mu = 4.632 \times 10^{-16}$ emu. Again, using the bulk saturation magnetization value of cobalt at 0 K, M_{bulk} = 1435 emu cm^{-3}.[14] We estimated a particle diameter of 8.5 nm.

In summary, we attempted to prepare a Kekulé diradicaloid with a perfluoronaphthalene spacer, but we realized an unprecedented 18-electron Co(I) species **5**, where the two *meta* fluorines of the hexafluoronaphthyl ring were substituted with $CoCp_2$ and formed an unusual C–C bond through one of the Cp rings.

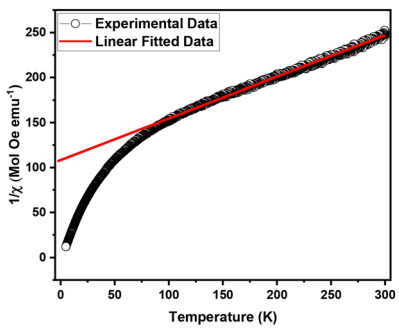

Fig. 5 The inverse susceptibility data of **5** and its fitting with Curie–Weiss law.

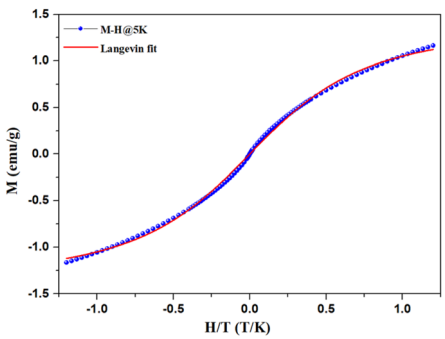

Fig. 6 Magnetization *versus* H/T at 5 K and its fitting to Langevin function for compound **5**.

Author contributions

GK: conceptualization, synthesis, structural studies, formal analysis, writing original draft, DP: methodology, data curation, SRD: theoretical studies, writing original draft, RK: theoretical studies, MS: magnetic studies, ST: structural studies AG: supervision-theoretical studies, KV: supervision-theoretical studies, KS: supervision-magnetic studies, SSS: conceptualization, funding acquisition, supervision, writing – review and editing.

Data availability

The data supporting this article have been included as part of the ESI.† CCDC 2270083 (**3·2HF$_2$**), 2270084 (**3·2B$_2$F$_7$**) and 2270085 (**5**)† can be obtained from **https://www.ccdc.cam.ac.uk/structures/**.

Conflicts of interest

There are no conflicts to declare.

Acknowledgements

S. S. S. is thankful for SJF Grant SB/SJF/2021-22/06, GOI for providing financial assistance. G. K. and R. K. thank CSIR, India for their research fellowships. D. P. thanks UGC-India for his research fellowships. A. G. acknowledges financial support from SERB (SRG/2022/001115). ST thanks SERB, New Delhi, India, for funding Start-up Research Grant (SRG/2023/000209) and AESD&CIF (MLP0072), CSIR-CSMCRI, Bhavnagar, India for the infrastructure.

References

1 (*a*) R. S. Ghadwal, D. Rottschäfer, B. Neumann, H.-G. Stammler, M. v. Gastel and D. Andrada, *Angew. Chem., Int. Ed.*, 2018, **57**, 4855–4859; (*b*) R. S. Ghadwal, D. Rottschäfer, B. Neumann, H. G. Stammler and D. M. Andrada, *Chem. Sci.*, 2018, **9**, 4970–4976; (*c*) D. Rottschäfer, J. Busch, B. Neumann, H. G. Stammler, M. v. Gastel, R. Kishi, M. Nakano and R. S. Ghadwal, *Chem. – Eur. J.*, 2018, **24**, 16537–16542.

2 (*a*) A. Maiti, J. Stubbe, N. I. Neuman, P. Kalita, P. Duari, C. Schulzke, V. Chandrasekhar, B. Sarkar and A. Jana, *Angew. Chem., Int. Ed.*, 2020, **59**, 6729–6734; (*b*) A. Maiti, S. Chandra, B. Sarkar and A. Jana, *Chem. Sci.*, 2020, **11**, 11827–11833; (*c*) A. Maiti, S. Sobottka, S. Chandra, D. Jana, P. Ravat, B. Sarkar and A. Jana, *J. Org. Chem.*, 2021, **86**, 16464–16472.

3 G. Kundu, S. De, S. Tothadi, A. Das, D. Koley and S. S. Sen, *Chem. – Eur. J.*, 2019, **25**, 16533–16537.

4 G. Kundu, S. R. Dash, R. Kumar, K. Vanka, A. Ghosh and S. S. Sen, *ChemPlusChem*, 2023, **88**, e202300273.

5 M. M. Hansmann, M. Melaimi, D. Munz and G. Bertrand, *J. Am. Chem. Soc.*, 2018, **140**, 2546–2554.

6 B. Barry, G. Soper, J. Hurmalainen, A. Mansikkamäki, K. N. Robertson, W. L. McClennan, A. J. Veinot, T. L. Roemmele, U. Werner-Zwanziger, R. T. Boeré, H. M. Tuononen, J. Clyburne and J. D. Masuda, *Angew. Chem., Int. Ed.*, 2018, **57**, 749–754.

7 Y. K. Loh, P. Vasko, C. McManus, A. Heilmann, W. K. Myers and S. Aldridge, *Nat. Commun.*, 2021, **12**, 7052.

8 (*a*) J. Guo, Z. Li, X. Tian, T. Zhang, Y. Wang and C. Dou, *Angew. Chem., Int. Ed.*, 2023, **62**, e202217470; (*b*) J. E. Barker, T. W. Price, L. J. Karas, R. Kishi, S. N. MacMillan, L. N. Zakharov, C. J. Glmez-García, J. I. Wu, M. Nakano, M. M. Haley and J. Casado, *J. Am. Chem. Soc.*, 2020, **142**, 20444–20455.

9 (*a*) W. Kueh, X. Shi, T. W. Phua, H. Kueh, Y. C. Liau and C. Chi, *Org. Lett.*, 2022, **24**, 5935–5940; (*b*) J. E. Barker, C. K. Frederickson, M. H. Jones, L. N. Zakharov and M. M. Haley, *Org. Lett.*, 2017, **19**, 5312–5315.

10 (*a*) N. Kuhn, J. Fahl, R. Boese and G. Henkel, *Z. Naturforsch., B: J. Chem. Sci.*, 1998, **53**, 881–886; (*b*) E. Mallah, N. Kuhn, C. Maichle-Moβmer, M. Steimann, M. Ströbele and K.-P. Zeller, *Z. Naturforsch.*, 2009, **64b**, 1176–1182; (*c*) Y. Kim and E. Lee, *Chem. Commun.*, 2016, **52**, 10922–10925; (*d*) U. S. D. Paul and U. Radius, *Chem. – Eur. J.*, 2017, **23**, 3993–4009; (*e*) J. Emerson-King, S. A. Hauser and A. B. Chaplin, *Org. Biomol. Chem.*, 2017, **15**, 787–789; (*f*) S. Styra, M. Melaimi, C. E. Moore, A. L. Rheingold, T. Augenstein, F. Breher and G. Bertrand, *Chem. – Eur. J.*, 2015, **21**, 8441–8446; (*g*) M. Pait, G. Kundu, S. Tothadi, S. Karak, S. Jain, K. Vanka and S. S. Sen, *Angew. Chem., Int. Ed.*, 2019, **58**, 2804–2808; (*h*) G. Kundu, V. S. Ajithkumar, M. K. Bisai, S. Tothadi, T. Das, K. Vanka and S. S. Sen, *Chem. Commun.*, 2021, **57**, 4428–4431.

11 (*a*) F. Lu, H. Sun and X. Li, *Chin. J. Chem.*, 2013, **31**, 927–932; (*b*) D. Ertler, M. W. Kuntze-Fechner, S. Dürr, K. Lubitz and U. Radius, *New J. Chem.*, 2021, **45**, 14999–15016; (*c*) J. Li, T. Zheng, H. Sun, W. Xu and X. Li, *Dalton Trans.*, 2013, **42**, 5740–5748.

12 M. M. Hansmann, M. Melaimi and G. Bertrand, *J. Am. Chem. Soc.*, 2017, **139**, 15620–15623.

13 A. Kumar, Meenakshi and R. N. Mahato, *J. Supercond. Novel Magn.*, 2019, **32**, 3947–3955.

14 M. E. McHenry, S. A. Majetich, J. O. Artman, M. DeGraef and S. W. Staley, *Phys. Rev. B: Condens. Matter Mater. Phys.*, 1994, **49**, 11358–11363.